Research Square

Preprints are preliminary reports that have not undergone peer review. They should not be considered conclusive, used to inform clinical practice, or referenced by the media as validated information.

Chemical vapor deposition of tungsten-based layers on detonation coatings

Evgeny Ruban

evgeny.ruban991@gmail.com

Frumkin Institute of Physical Chemistry and Electrochemistry Russian Academy of Sciences

Sergey Vashin

Frumkin Institute of Physical Chemistry and Electrochemistry Russian Academy of Sciences

Stepan Rachko

Frumkin Institute of Physical Chemistry and Electrochemistry Russian Academy of Sciences

Sergey Rybakov

Frumkin Institute of Physical Chemistry and Electrochemistry Russian Academy of Sciences

---

Research Article

Keywords: detonation spraying coatings, chemical vapor deposition, tungsten coating, tungsten hexafluoride WF6

Posted Date: October 19th, 2026

DOI: https://doi.org/10.21203/rs.3.rs-11244194/v1

License: This work is licensed under a Creative Commons Attribution 4.0 International License. Read Full License

Additional Declarations: No competing interests reported.

Chemical vapor deposition of tungsten-based layers on detonation coatings

Evgeny Ruban*, Sergey Vashin, Stepan Rachko, Sergey Rybakov

Frumkin Institute of Physical Chemistry and Electrochemistry Russian Academy of Sciences, 31-4, Leninsky prospect, 119071 Moscow, Russia.

*Corresponding author, e-mail: evgeny.ruban991@gmail.com

Received XX.XX.2026

Abstract

In this study, detonation coatings were preapplied as adhesive intermediate layers obtained from WC-Co, WC-Ni(10), WC-Ni(20), WC-Co-Cr and NiCr-Cr_3C_2 powders. Tungsten hexafluoride WF_6 is used for chemical vapor deposition of tungsten coatings. The dispersed composition of the powders was studied via laser diffraction, the phase composition of the powders and coatings obtained from them via X-ray diffraction, and chemical element analysis via EDS. The powder shape and the "detonation coating/tungsten coating" and "detonation coating/substrate" interfaces were examined by scanning electron microscopy. The combined use of detonation spraying and chemical vapor deposition allows the distributed deposition of tungsten coatings on a steel substrate from the detonation coating sublayer and regulates the porosity of the surface of detonation coatings by depositing a layer of tungsten on them via chemical vapor deposition.

Keywords: detonation spraying coatings, chemical vapor deposition, tungsten coating, tungsten hexafluoride WF_6

Introduction

The general causes of failure of industrial equipment components and parts are friction and abrasive types of wear [1]. Various types of surface treatment are used to increase wear resistance: chemical and thermal treatment [2], thermal spraying coatings (HVOF, HVAF, laser cladding, and plasma spraying), physical vapor deposition (PVD) (magnetron, ion and vacuum types of deposition), chemical vapor deposition (CVD), laser melting, arc deposition, and galvanic coatings, as well as hardness and superhard alloys, and the introduction of special alloying additives into their composition (tungsten, molybdenum, chromium, ceramic species, etc.) [3-5].

A flexible approach is to use hardness wear-resistant coatings, which are available via a limited number of methods. Chromium-based hardness galvanic coatings are good examples for wear-resistant applications [6], but the high degree of toxicity of the chrome plating process limits their use [7]. The hardness of compound layers produced via physical vapour deposition methods is difficult to obtain with equal compositions and thicknesses of complex products [8]. Thermal spraying coatings are widely used [9], but they have high porosity, which is unacceptable for most applications, and contain a multiphase structure, which reduces their operational properties [10]. Tungsten-based CVD coatings, including tungsten carbides [11, 12], cannot be directly deposited on steel surfaces [13].

Combining hardness coating technologies to obtain the best quality product for industrial practical application is an extremely urgent task. The approach of depositing PVD layers onto a WC-Co-system hard alloy substrate has already been applied [14-18]. Detonation-gaseous spraying (D-gun), which is one of the methods of thermal spraying, allows the application of coatings that preserve the original phase-element composition of the original powders, with good adhesion to the surface, uniformity and equal thickness without surface heat treatment, including on internal surfaces (with some restrictions). The combination of D-gun and CVD makes it possible to provide porosity closure via CVD layers for D-gun coatings and, conversely, to provide adhesion contact CVD coatings for steel subscribed underlayer D-gun coatings. This research is dedicated to matching the same layers.

Experimental

The detonation-gaseous spraying of metal and ceramic powders was implemented via the D-gun automatic technologic complex ADU “Ob” (NTC Detonatsiya, Russia) [19]. Acetilene C_2H_2 (pure A, NII KM, Russia) was used as a gas fuel, and the oxidant was gaseous oxygen O_2 (99.99%, NII KM, Russia). Sample surfaces were previously cleaned of dirt and scale with activation immediately before being sprayed with quartz sand via air abrasive treatment (species scale 0.5–1.5 mm) [20-22].

Tungsten layers were obtained via CVD in a vacuum reactor with a heat side with the tungsten precursor tungsten hexafluoride WF_6 (99.99%, NPO Luch, Russia) and a reduction in gaseous hydrogen H_2 (99.999 %, NII KM, Russia). Highly active chemical transformation products were deactivated by spraying aqueous alkaline solution in a scrubber, which was installed in series after the rotary vane vacuum pump [23].

Samples preparation (steels St3 or St45 20x30x3 mm^3) were performed via a metallographic cutting machine, MICRACUT 202 (Metkon, USA), with subsequent

production of a metallographic section on a pressing machine, ECOPRESS 52 (Metkon, USA), and grinding and polishing on an automatic grinding and polishing machine, FORCIPOL 102 (Metkon, USA).

The powders granulometric composition were measured on a particle size analyser via a laser diffraction Mastersizer 2000 M (Malvern Instruments, GB) via an automatic liquid dispersion and a sample feeding module Hydro 2000S [24-26]. Powder flowability and bulk density were investigated via the weight method via a Hall funnel [27, 28].

The D-gun powders used were No. 1 – WC-Co(17) (Sulzer Metco, USA), No. 2 – WC-Ni(10) (n/n, CPR), No. 3 – WC-Ni(20) (Technikord, Russia), No. 4 – WC-Co-Cr (Gorizont pokritiy, Russia), and No. 5 – NiCr-Cr_3C_2 (HTC, CPR).

Powders morphology and particle size analysis were carried out on an ICOE CB800PRT optical microscope (Synercon, Russia) in bright field mode [29-31]. The microstructure and thickness of the coatings were investigated via a metallographic inverted microscope (ICOE MIV5500D; Synercon, Russia) according to standard methods [32].

Powder and coating phase element analyses were performed via X-ray phase analysis (XRD) on an X-ray diffractometer (Tongda TD-3700; Dandong Tongda, КНР) with CuKα radiation. The results of the experiment were processed via QualX software.

Powder species and multilayer coating microstructures were investigated by scanning electron microscopy (SEM) SM-32A (Melytec, CPR) with an X-ray detector Xplore 30 (Oxford Instruments, GB) for energy dispersive analysis (EDX) to study the elemental chemical composition of the powders and coatings [33, 34]. The accumulation and processing of X-ray spectra were performed with AZtecOne software.

Results and discussion

Powders investigation

The average bulk diameter of species and specific surface area for powder No. 1 are 43.62 μm and 0.162 m^2/g, respectively; No. 2, 49.78 μm and 0.254 m^2/g; No. 3, 32.39 μm and 0.387 m^2/g; No. 4, 32.42 μm and 0.197 m^2/g; and No. 5, 38.76 μm and 0.168 m^2/g.

Powder No. 1 (Fig. 1,a) contains particles of an elongated shape that are close to spherical. The particles of powder No. 1 mostly have a spherical shape of approximately the same geometric dimensions; as a result of the particle spheroidization operation, no dust fraction was detected. The single powder particles consisted of sintered polycrystals of submicron size. Powder No. 2 (Fig. 1,b) contains species with predominantly spherical

shapes, and ultrafine particles of submicron sizes that do not participate in the coating spraying process burn when the detonation products are fired. Powder particle No. 2 has a spherical shape with no signs of agglomeration; the particles themselves consist of WC tungsten carbide crystals interconnected by nickel bonds. Owing to the application of the particle spheroidization operation, WC crystallites have rounded fused faces. Powder No. 3 (Fig. 1,c) contains mainly particles of complex multifaceted shapes, as well as many ultrafine particles of submicron sizes. Powder particles No. 3 have arbitrary polyhedral shapes with geometric dimensions in a wide range. Apparently, the powder was not subjected to any postprocessing (screening, size concentration, spheroidization, etc.). Powder No. 4 (Fig. 1, d) consists mainly of spherical species with a low dust fraction. The particles of powder No. 4 have a spherical shape, which is obtained as a result of the particle spheroidization operation, and have similar geometric dimensions. No dust fraction was detected. The single powder particles consisted of sintered polycrystals of submicron size. No. 5 (Fig. 1, e) is mainly represented by spherical species, and there are enlarged agglomerates of species. Powder No. 5 is predominantly spherical in shape with agglomeration of smaller submicron particles with larger microscale sizes, and the surface of the powder species is represented by individual crystallites without sharp angles that are "fused" during spheroidization.

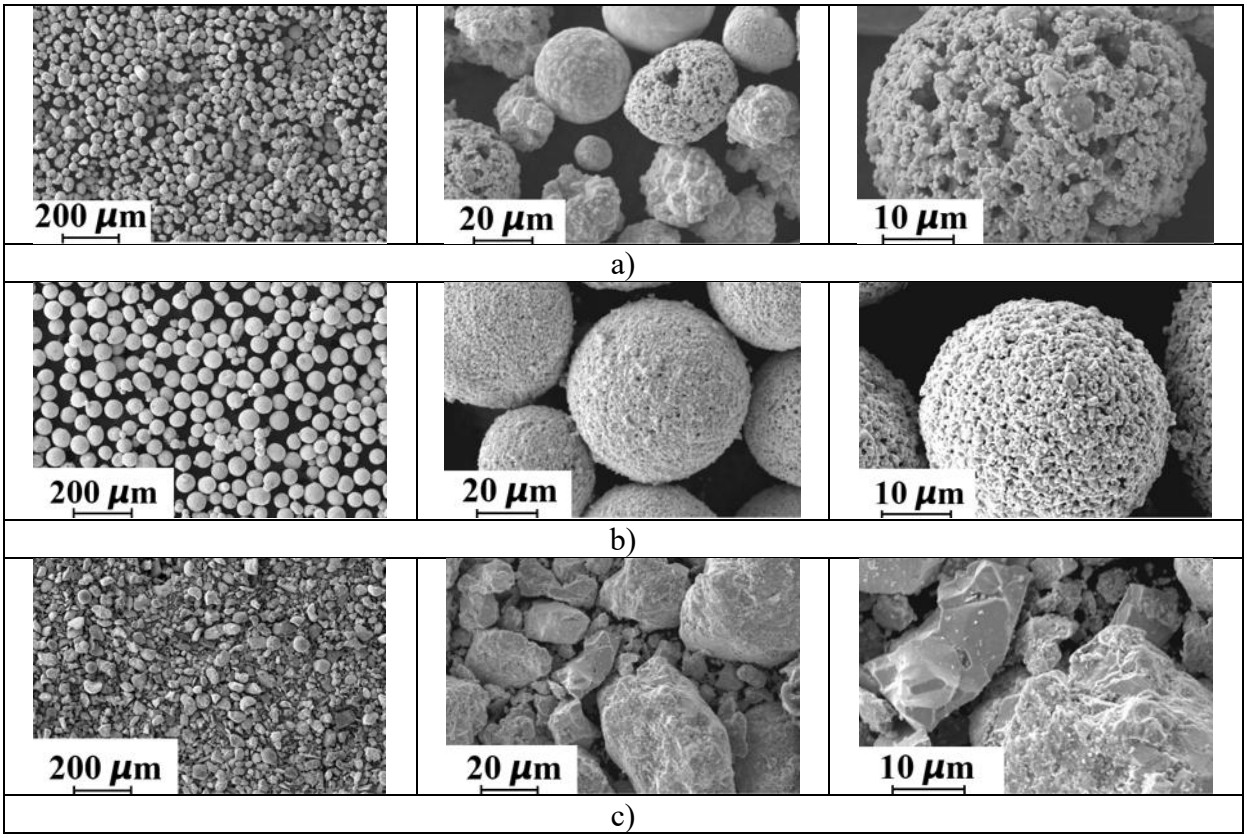

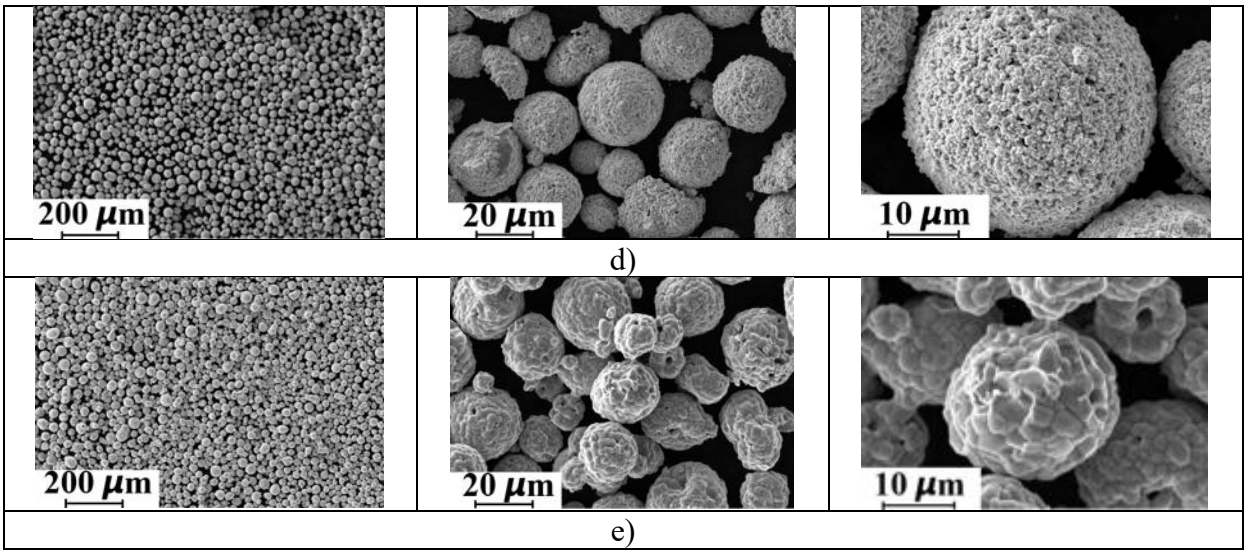

Fig. 1. SEM images of powder samples: a) No. 1, b) No. 2, c) No. 3, d) No. 4, e) No. 5

Powder No. 1 (Fig. 2a) consists of W, Co, C, O and Cr 65.93/23.17, 22.92/25.13, 6.10/32.79, 4.51/18.23 and 0.55/0.68 wt.%/at.%, respectively. Powder No. 2 (Fig. 2,b) consists of W, C and Ni at 82.36/23.59, 9.45/57.26 and 8.18/10.14 wt.%/at.%, respectively. Powder No. 3 (Fig. 2,c) contains W, Ni, C, Cr, O, Fe and Co 45.37/12.50, 29.31/25.30, 9.49/40.03, 6.11/5.95, 3.34/10.58, 3.25/2.95 and 3.14/2.70 wt.%/at.%, respectively. The presence of Fe, Co, Cr and O impurities in the powder composition indicates the ingress of materials from the lining of pipelines and assemblies of technological machines, most likely represented by stainless steels containing these elements, during the powder production process owing to the higher hardness of the phases in the processed powder materials and their dry abrasive action, as well as the absence or insufficient organization of quality control of manufactured powder products. Powder No. 4 (Fig. 2, d) consists of W, C, Co, O and Cr at 79.00/26.99, 10.63/55.58, 6.22/6.62, 2.13/8.36 and 2.02/2.44 wt.%/at.%, respectively. Powder №5 (Fig. 2e) consists of Cr, C, Ni and W at 76.17/49.93, 16.30/46.24, 6.16/3.58 and 1.37/0.25 wt.%/at.%, respectively.

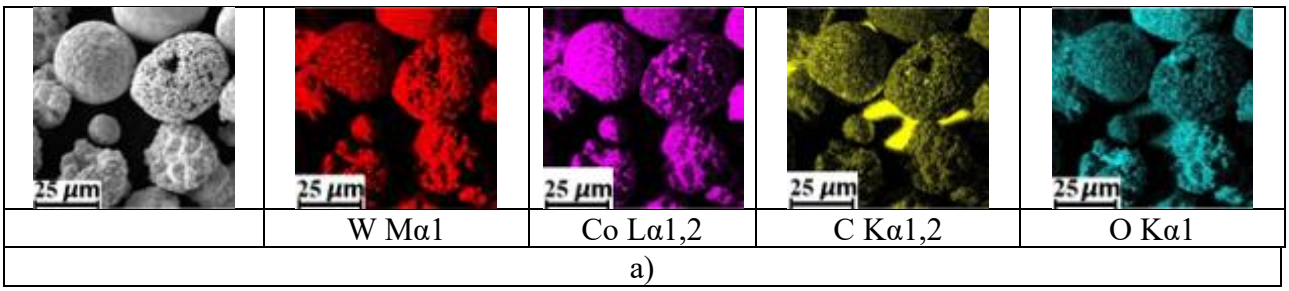

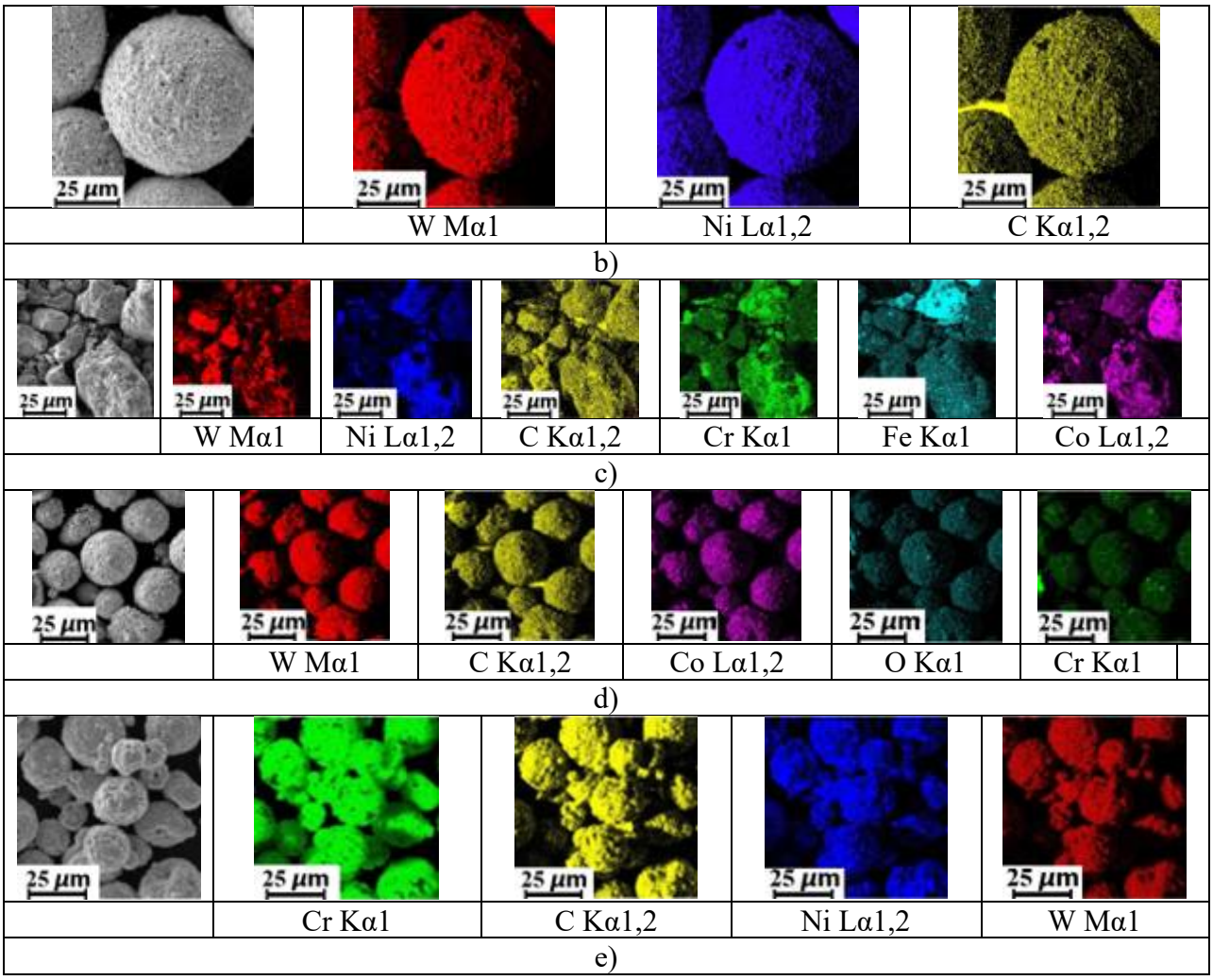

Fig. 2. Distribution of elements over the surface of powder particles: a) No. 1, b) No. 2, c) No. 3, d) No. 4, e) No. 5

Detonation- gaseous spraying coatings

The detonation coatings produced by spraying technology are shown in Table 1.

Table. 1. D-gun coating spraying technique

No.	Composition	*L*, mm	*FF*, %	O_2/C_2H_2	*h*, *μ*m	*υ*, mm/min
1	WC-Co(17)	150	48	1.08	5	2000
2	WC-Co-Cr	150	48	1.07	5	2000
3	NiCr-Cr_3C_2	160	27	1.1	5.5	1800
4	WC-Ni(10)	150	47	1.08	6	2100
5	WC-Ni(20)	160	45	1.08	5.5	2000

L – distance from the trunk section to the sprayed plane, mm; *FF* – barrel fill factor, %; *h* – thickness of a single layer, *μ*m; *υ* – speed of movement of the manipulator, mm/min.

Coating No. 1 (Fig. 3a) is characterized by a dense uniform microstructure with an observed regular microporosity. The “coating/substrate” interface border has no peeling throughout, which indicates sufficient coating adhesion on the surface. Coating No. 2 (Fig. 3,

b) is characterized by a porous microstructure with the possibility of forming pores according to its coating bulk in the presence of satisfactory coating adhesion on the substrate surface, as expressed by the absence of peeling of the coating sections. Coating No. 3 (Fig. 3,c) has a dense, homogeneous microstructure with a minimum number of micron-scale pores. The “coating/substrate” interface border has distinct halos with the possibility of forming “shells” that do not noticeably affect the adhesion of the sprating layer. In coating No. 4 (Fig. 3, d), irregular cracks are observed, which in turn do not lead to deterioration of coating adhesion or detachment. The coating microstructure is quite homogeneous, with the possibility of the appearance of closed pores at the micron scale in the near-surface coating layer. Coating No. 5 (Fig. 3e) has a “loose” microstructure with the possibility of forming an open, branched porosity on the coating bulk. The “coating/substrate” interface border has no signs of peeling.

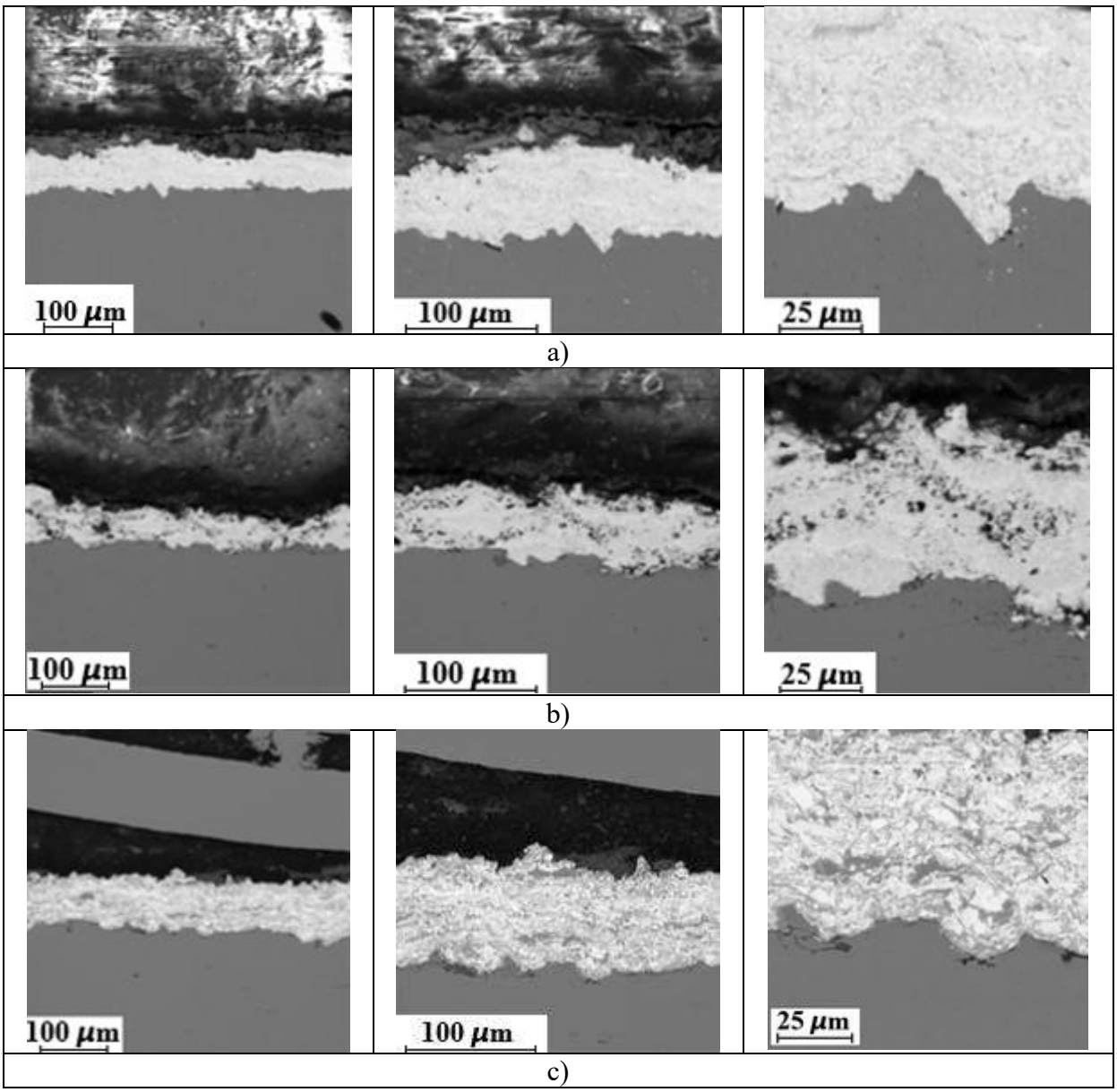

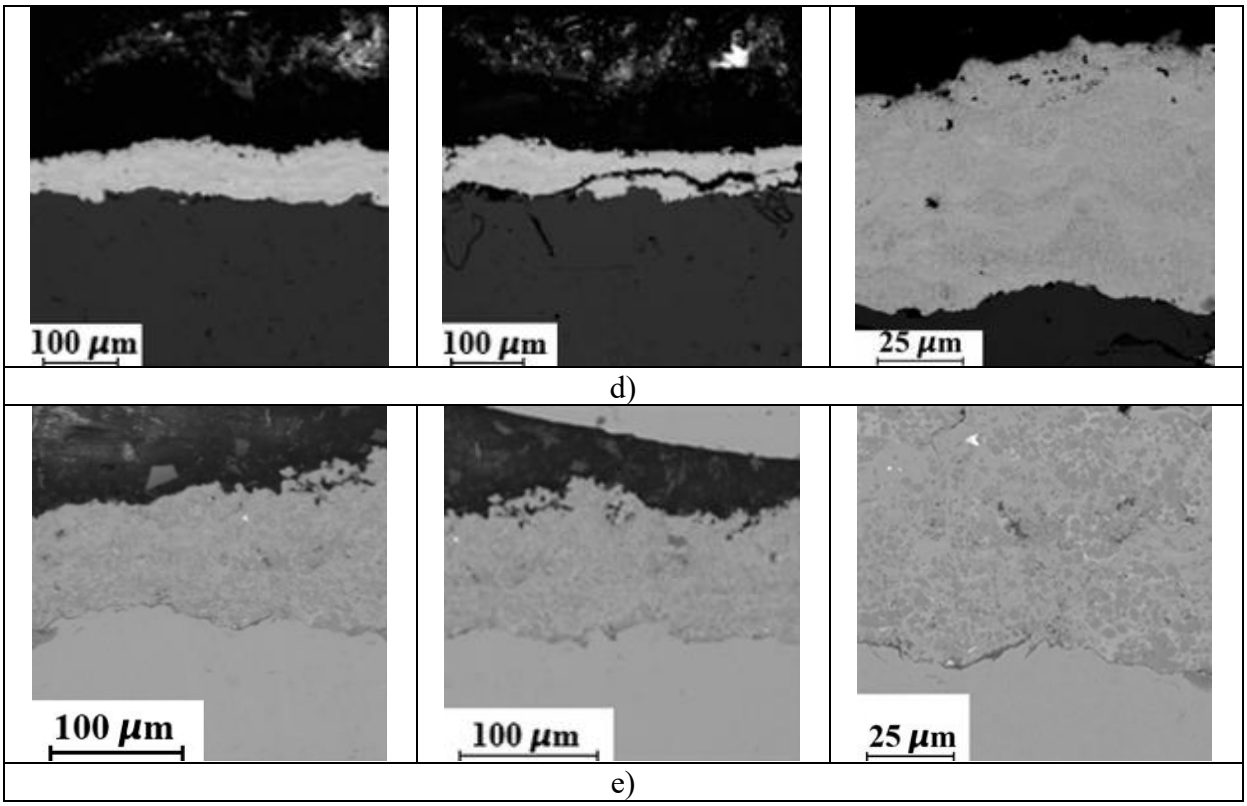

Fig. 3. SEM images of D-gun coatings: a) No. 1, b) No. 2, c) No. 3, d) No. 4, e) No. 5

Coating No. 1 (Fig. 4a) containing phases of WC and Co, which are contained in the initial powder, and α-W results in dissociated tungsten carbide (WC) during D-gun spraying. Coating No. 2 (Fig. 4,b) contains phases of WC and Ni, which are present in the original powder, and W_2C and W result in the dissociation of tungsten carbide WC during D-gun spraying. Coating No. 3 (Fig. 4,c) contains phases of WC and Ni, which are contained in the initial powder, and W_2C, W results in dissociated tungsten carbide (WC) during D-gun spraying. Coating No. 4 (Fig. 4, d) contains phases of WC and Co, which are contained in the initial powder, and W_2C results in the dissociation of tungsten carbide WC during D-gun spraying. The Cr phase, which is present in the original powder, was not detected in the coating; most likely, chromium partially burned out at low temperatures, and its small amount in the spraying coating could not be detected by XRD because of the detection limit of the compounds by a diffractometer. Coating No. 5 (Fig. 4e) contains the phases Cr, NiCr and Ni, which are contained in the initial powder, as well as Cr_3C_2 and Cr_2O_3, which are formed during spraying coating.

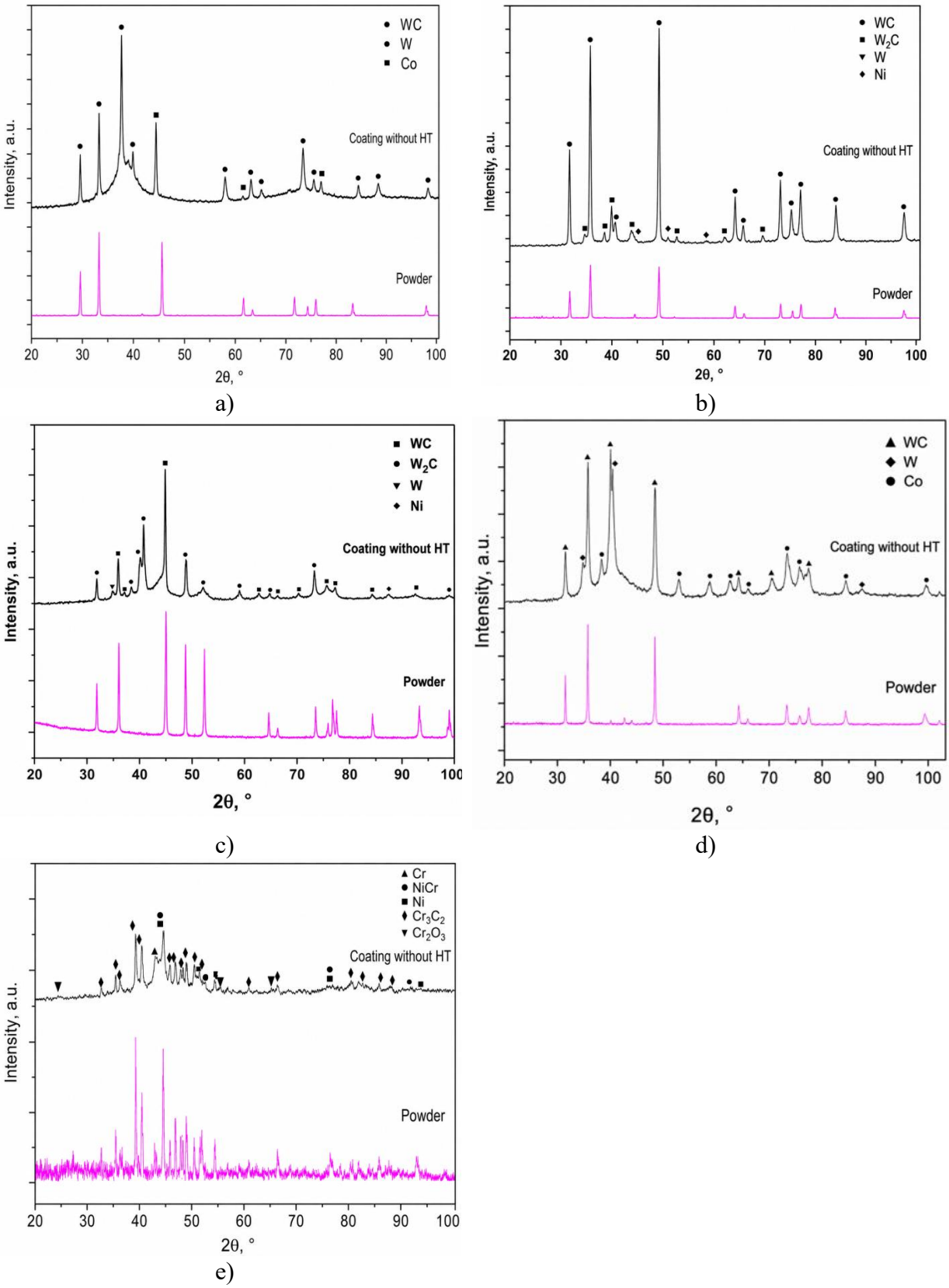

Fig. 4. Powders and D-gun coatings diffractograms: a) No. 1, b) No. 2, c) No. 3, d) No. 4, e) No. 5

CVD tungsten coatings

CVD tungsten coatings were obtained via the following methods: 1 l/h WF_6, 5.5 l/h H_2, a precipitation temperature of 530 °C, a pressure of 180 ± 10 Torr, and precipitation for 40 min.

The two-layer WC-Co coating with deposited tungsten has a uniform microstructure, the "substrate-detonation coating" boundary is clearly visible, and the "detonation coating-CVD coating" boundary is distinguishable by the presence of a denser outer CVD layer of tungsten. Submicron-sized pores are also discernible in the detonation layer. The microstructure of the detonation layer contains some porosity with submicron–micron dimensions (Fig. 4a). Two-layer WC–Ni(10) coatings with deposited tungsten have a uniform phase distribution in the detonation layer, and the boundaries of the layers are distinguishable. The closure of the surface porosity in the detonation layer by the deposited CVD layer of tungsten is also noticeable (Fig. 4,b). The two-layer WC-Ni(20) coating with deposited tungsten has distinguishable "substrate-detonation coating" and "detonation coating-CVD coating" boundaries, and no porosity was visually detected in the coating layers (Fig. 4,c). The two-layer WC-Co-Cr coating with deposited tungsten has a clear "substrate-detonation coating" boundary, and the CVD layer of tungsten on the detonation layer has a small thickness and is distinguishable on the outer surface of the sample because of the denser microstructure of tungsten (Fig. 4,d). The two-layer NiCr-Cr_3C_2 coating with deposited tungsten has a clearly distinguishable boundary "substrate-detonation coating" and "detonation coating-CVD coating" (Fig. 4e).

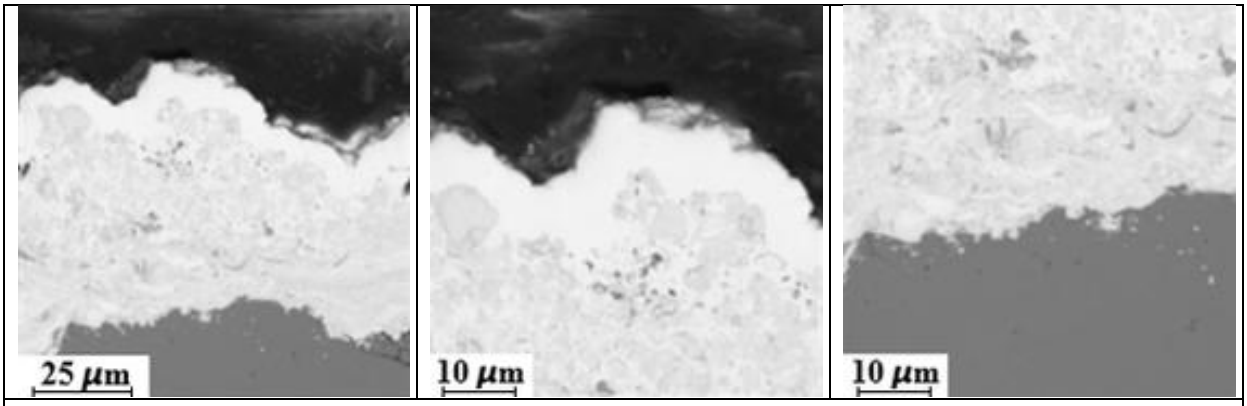

a)

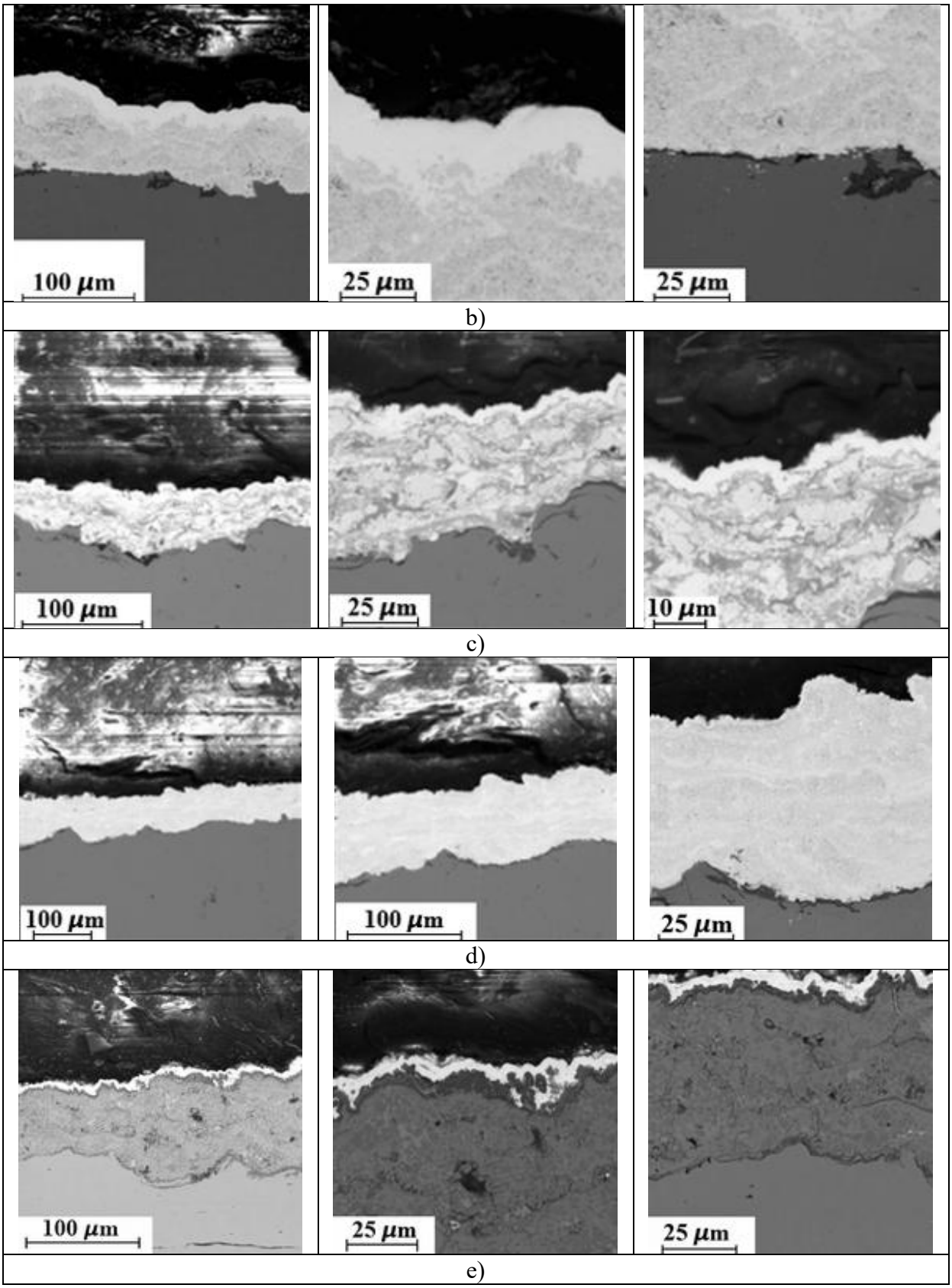

Fig. 5. SEM images of D-gun coatings with deposited W coatings: a) WC-Co/W, b) WC-Ni(10)/W, c) WC-Ni(20)/W, d) WC-Co-Cr/W, e) NiCr-Cr_3C_2/W

The two-layer WC-Co/W coating contains W with a uniform thickness distribution, and Co is less evenly distributed: the concentration decreases slightly towards the sample surface, and carbon in the D-gun layer is poorly expressed owing to its identification features. The outer CVD layer of tungsten is distinguishable on the surface of the sample (Fig. 5a). The WC–Ni(10)/W coating consists of W, Ni and C with a uniform thickness distribution. The outer CVD layer of tungsten is distinguishable on the surface of the sample (Fig. 5,b). The WC-Ni(20)/W coating consists of W, Ni and C with a uniform thickness distribution. The outer CVD layer of tungsten is distinguishable on the surface of the sample (Fig. 5,c). The WC-Co-Cr/W coating contains W, Co, and Cr with a uniform thickness distribution; carbon in the D-gun layer is poorly expressed because of its identification features. The outer CVD layer of tungsten is distinguishable on the surface of the sample (Fig. 5,d). The NiCr-Cr_3C_2/W coating contains Ni, C and Cr with a uniform thickness distribution. The outer CVD layer of tungsten is clearly visible on the surface of the sample (Fig. 5,e).

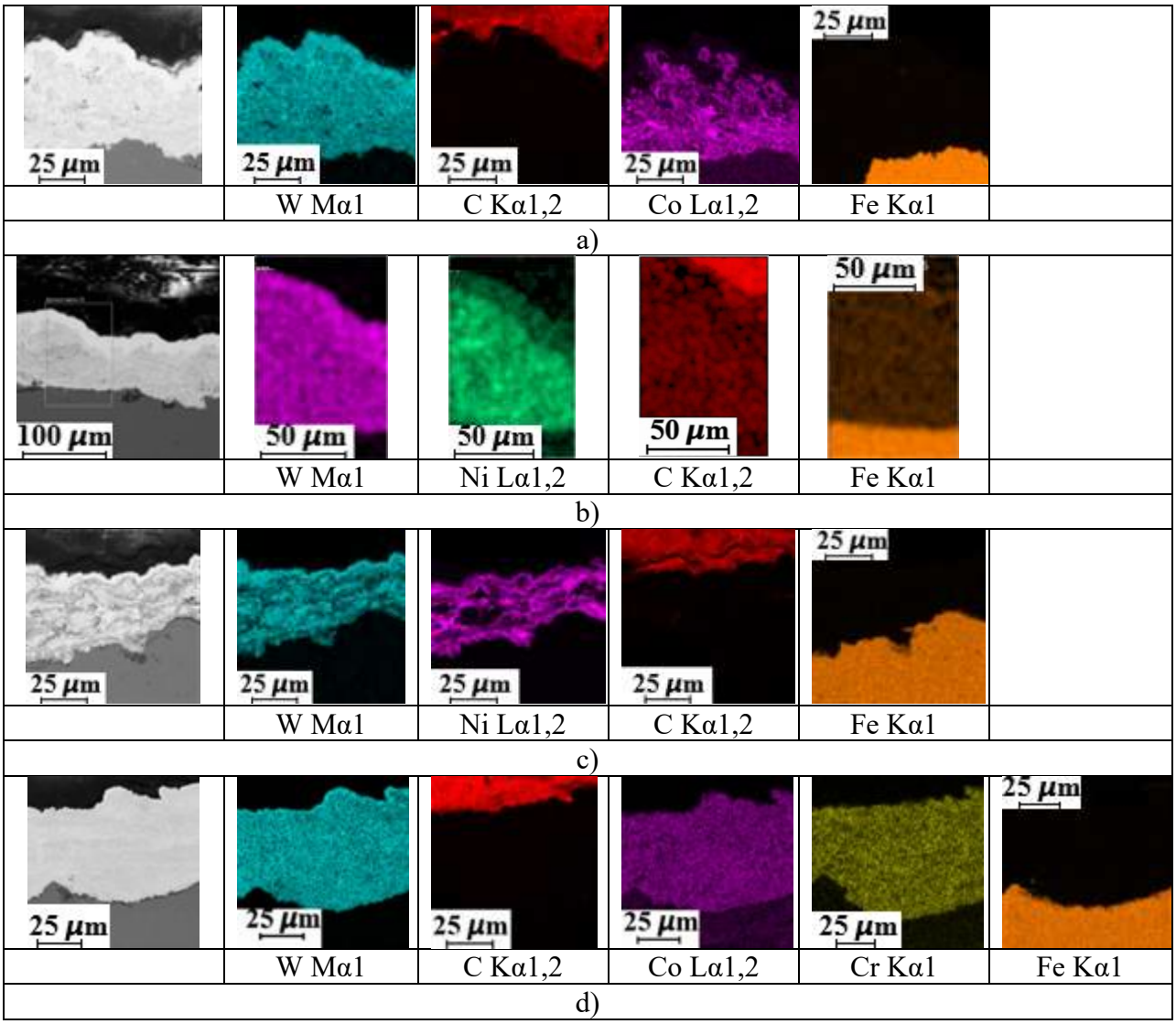

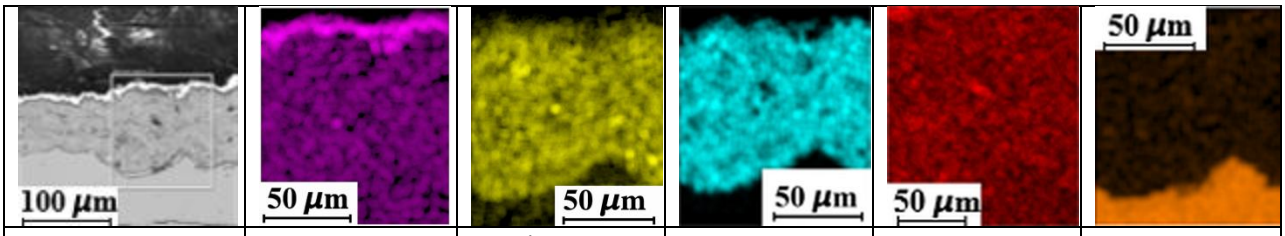

	W Mα1	Ni Lα1,2	Cr Kα1	C Kα1,2	Fe Kα1
e)					

Fig. 6. Distribution of elements on various metallographic detonation coatings and deposition of CVD layers of tungsten on a) WC-Co/W, b) WC-Ni(10)/W, c) WC-Ni(20)/W, d) WC-Co-Cr/W, e) NiCr-Cr_3C_2/W

Conclusions

The chemical vapour deposition of a tungsten coating from tungsten hexafluoride WF_6 onto detonation coatings composed of WC-Co, WC-Ni(10), WC-Ni(20), WC-Co-Cr and NiCr-Cr_3C_2 sprayed onto a steel substrate was considered. Owing to the lack of adhesion between WF_6 CVD coatings and steel surfaces, detonation coatings can act as intermediate adhesive support layers on which tungsten CVD coatings can be obtained. This was confirmed by SEM, XRD, and EDS analyses of the obtained two-layer coating systems. The "substrate-detonation coating" and "detonation coating-tungsten coating" interfaces clearly have distinguishable boundaries. Notably, owing to the porosity of the detonation coatings resulting from the spraying process, it is possible to close part of the surface porosity by depositing a tungsten CVD coating. This effect of decreasing the porosity of CVD detonation coatings with a tungsten coating can be used to increase the corrosion resistance and wear resistance of coated parts and to obtain a smoother surface morphology without the need for rough machining.

Funding: This work was supported by the Ministry of Science and Higher Education of the Russian Federation (No. 075-15-2025-583).

Declarations

Conflict of interest The authors declare that they have no known competing financial interests or personal relationships that could have appeared to influence the work reported in this paper.

References

1. A. Patnaik, T. Singh, and V. Kukshal (2021) Tribology in Materials and Manufacturing: Wear, Friction and Lubrication, BoD—Books on Demand, Norderstedt, 333 p. ISBN-13: 978-1838805579.

2. H. Li, J. Chen, W. Zhang, H. Zhan, C. He, Z. Yang, H. Peng, and L. Leng (2023) Machine-Learning-Aided Thermochemical Treatment of Biomass: A Review, Biofuel Res. J., 10(1), 1786–1809. doi: 10.18331/BRJ2023.10.1.4

3. P. Sarvar and H. Firuz, Hard Alloy Applications (2023), Universum: Tekhnicheskie Nauki, 8-4(113), 4–7 (in Russian). doi: 10.32743/UniTech.2023.113.8.15860

4. V. Kanyanta (2016) Hard, Superhard and Ultrahard Materials: An Overview, in Microstructure-Property Correlations for Hard, Superhard, and Ultrahard Materials, Springer, Cham, 1–23. doi: 10.1007/978-3-319-29291-5_1

5. Y. Wang, C. Feng, T. Lin, R. Zhu, J. Zhang, H. Yang, S. Yi, J. He, M. Tu, and G. Wei (2025) A Review of Wear-Resistant Coatings for Steel Substrates: Applications and Challenges, Metals, 15(11), 1231. doi: 10.3390/met15111231

6. N.V. Mandich and D.L. Snyder (2010) Electrodeposition of Chromium, in Modern Electroplating, 5th ed., M. Schlesinger and M. Paunovic, Eds., Wiley, Hoboken, NJ, 205–241. doi: 10.1002/9780470602638.ch12

7. S. Wang, C. Ma, and F.C. Walsh (2020) Alternative Tribological Coatings to Electrodeposited Hard Chromium: A Critical Review, Trans. IMF, 98(4), 173–185. doi: 10.1080/00202967.2020.1776962

8. B. Navinšek, P. Panjan, and I. Milošev (1999) PVD Coatings as an Environmentally Clean Alternative to Electroplating and Electroless Processes, Surf. Coat. Technol., 116–119, 476–487. doi: 10.1016/S0257-8972(99)00145-0

9. Anon., Thermal Spray Service Market, Global Market Insights, https://www.gminsights.com/industry-analysis/thermal-spray-service-market. Accessed 4 April 2026.

10. H. Fukanuma (1994) A Porosity Formation and Flattening Model of an Impinging Molten Particle in Thermal Spray Coatings, J. Therm. Spray Technol., 3(1), 33–44. doi: 10.1007/BF02648997

11. V.V. Dushik, N.V. Rozhanskii, V.O. Lifshits, T.V. Rybkina, and V.P. Kuzmin (2018) The Formation of Tungsten and Tungsten Carbides by CVD Synthesis and the Proposed Mechanism of Chemical Transformations and Crystallization Processes, Mater. Lett., 228, 164–167. doi: 10.1016/j.matlet.2018.06.003

12. H. Zhang, X. Yu, Z. Nie, C. Tan, F. Wang, H. Cai, Y. Li, F. Wang, and H. Cai (2018) Microstructure and Growth Mechanism of Tungsten Carbide Coatings by Atmospheric CVD, Surf. Coat. Technol., 344, 85–92. doi: 10.1016/j.surfcoat.2018.03.023

13. E.A. Ruban and S.Yu. Rachko (2026) Thermodynamic Calculation of the Interaction of the Components of a Gaseous Medium with the Substrate Surface During CVD of Tungsten-Based Coatings, Russian Journal of Physical Chemistry A, 100 (10), 2247–2252. doi: 10.1134/S0036024426701700

14. F.F. Komarov, V.M. Konstantinov, A.V. Kovalchuk, S.V. Konstantinov, and H.A. Tkachenko (2016) The Effect of Steel Substrate Prehardening on Structural, Mechanical, and Tribological Properties of Magnetron Sputtered TiN and TiAlN Coatings, Wear, 352–353, 92–101. doi: 10.1016/j.wear.2016.02.008

15. H.G. Prengel, P.C. Jindal, K.H. Wendt, A.T. Santhanam, P.L. Hegde, and R.M. Penich (2001) A New Class of High Performance PVD Coatings for Carbide Cutting Tools, Surf. Coat. Technol., 139(1), 25–34. doi: 10.1016/S0257-8972(00)01080-X

16. A. Inspektor and P.A. Salvador (2014) Architecture of PVD Coatings for Metalcutting Applications: A Review, Surf. Coat. Technol., 257, 138–153. doi: 10.1016/j.surfcoat.2014.08.068

17. Y. Long, J. Zeng, D. Yu, and S. Wu (2014) Microstructure of TiAlN and CrAlN Coatings and Cutting Performance of Coated Silicon Nitride Inserts in Cast Iron Turning, Ceram. Int., 40(7), 9889–9894. doi: 10.1016/j.ceramint.2014.02.083

18 B.M. de Freitas, D.S.L. Weiss, L.S. Santos, P. Soares, F.L. Amorim, J.M.F.P. Junior, C.A.H. Laurindo, and R.D. Torres (2025) Influence of Cobalt Content on the Adhesion of TiAlN and AlTiN/TiSiN Coatings on WC-Co Substrates, Surf. Interfaces, 72, 107339. doi: 10.1016/j.surfin.2025.107339

19. T.P. Gavrilenko, A.L. Kiryakin, Yu.A. Nikolaev, and V.Yu. Ulyanitskii (2006) Automated Detonation Complex “Ob” for Powder Coating Deposition, STA (Sovremennye Tekhnologii Avtomatizatsii), 4, 47–52 (in Russian).

20. Y.S. Borisov and Y.A. Kharlamov (1987) Thermal Spray Coatings from Powder Materials, Naukova Dumka, Kyiv, 210 p. (in Russian).

21. P.A. Vityaz, V.S. Ivashko, and E.D. Manuilo (1993) Theory and Practice of Flame Spraying, Navuka i Tekhnika, Minsk, 295 p. (in Russian). ISBN 5-343-01004-9.

22. V.V. Kudinov and V.M. Ivanov (1981) Plasma Deposition of Refractory Coatings, Mashinostroenie, Moscow, 192 p. (in Russian).

23. V.V. Dushik, E.A. Ruban, A.B. Drovosekov, A.A. Shaporenkov, and N.V. Rozhanskiy (2023) Synergetic Effect in Ni–P–W and W–C Multilayer Coating Systems Obtained by Chemical-Catalytic Metallization and Chemical-Vapor Deposition, J. Surf. Investig.: X-ray Synchrotron Neutron Tech., 17(6), 1364–1371. doi: 10.1134/S1027451023060265

24. GOST R 8.777-2011 (2011) State System for Ensuring the Uniformity of Measurements. Disperse Composition of Aerosols and Suspensions. Determination of Particle Size by Laser Diffraction, Standartinform, Moscow. (in Russian).

25. ISO 13320:2020 (2020) Particle Size Analysis -- Laser Diffraction Methods, International Organization for Standardization, Geneva.

26. ISO 21501-1:2025 (2025) Determination of Particle Size Distribution—Single Particle Light Interaction Methods—Part 1: Light Scattering Aerosol Spectrometer, International Organization for Standardization, Geneva.

27. GOST 20899-98 (1998) Metallic Powders. Determination of Flowability by Means of a Calibrated Funnel (Hall Flowmeter), Standartinform, Moscow. (in Russian).

28. GOST 19440-94 (1994) Metallic Powders. Determination of Apparent Density. Part 1: Funnel Method. Part 2: Scott Volumeter Method, Standartinform, Moscow. (in Russian).

29. GOST R 56169-2014 (2014) Optics and Optical Instruments. Operation Microscope. Requirements and Test Methods, Standartinform, Moscow. (in Russian).

30. GOST R ISO 17123-1-2011 (2011) State System for Ensuring the Uniformity of Measurements. Optics and Optical Instruments. Field Procedures for Testing Geodetic and Surveying Instruments. Part 1: Theory, Standartinform, Moscow. (in Russian).

31. ISO 9342-1:2023 (2023) Optics and Optical Instruments—Test Lenses for Calibration of Focimeters—Part 1: Reference Lenses for Focimeters Used for Measuring Spectacle Lenses, International Organization for Standardization, Geneva.

32. I. Novikov, V.S. Zolotorevskii, K.K. Portnoi, N.A. Belov, D.V. Livanov, S.V. Medvedeva, A.A. Aksenov, and Yu.V. Evseev (2009) Physical Metallurgy: Textbook. Vol. II, V.S. Zolotorevskii, Ed., MISiS Publishing House, Moscow, 528 p. (in Russian). ISBN 978-5-87623-247-2

33. K.F.J. Heinrich (1981) Electron Beam X-Ray Microanalysis, Van Nostrand Reinhold Company, New York, NY, 578. ISBN-10: 0442232861, ISBN-13: 978-0442232863

34. J.I. Goldstein, D.E. Newbury, P. Echlin, D.C. Joy, C. Fiori, and E. Lifshin (1984) Scanning Electron Microscopy and X-Ray Microanalysis, Mir, Moscow, 1, 303; 2, 351. (in Russian translation).